

5. T. Wang and K. Wu, Size-reduction and band-broadening design technique of uniplanar hybrid ring coupler using phase inverter for M(H)MIC's, *IEEE Trans Microwave Theory Tech* 47 (1999), 198–206.
6. N. Marchand, Transmission-line conversion transformer, *Electron* 17 (1944), 142–145.
7. S.A. Kian and I.D. Robertson, Analysis and design of impedance-transforming planar Marchand baluns, *IEEE Trans Microwave Theory Tech* 49 (2001), 402–406.
8. H.K. Chiou, J.W.R. Lian, and T.Y. Yang, A miniature Q-band balanced sub-harmonically pumped image rejection mixer, *IEEE Microwave Compon Lett* 17 (2007), 463–465.
9. M.C. Tsai, A new compact wideband balun, Vol. 1, In: *IEEE MTT-S International Microwave Symposium Digest*, Atlanta, GA, USA, June 1993, pp. 141–143.
10. P.S. Wu, C.H. Wang, T.W. Huang, and H. Wang, Compact and broad-band millimeter-wave monolithic transformer balanced mixers, *IEEE Trans Microwave Theory Tech* 53 (2005), 3106–3114.
11. J.W. Lee and K.J. Webb, Analysis and design of low-loss planar microwave baluns having three symmetric coupled lines, Vol. 1, In: *IEEE MTT-S International Microwave Symposium Digest*, Seattle, WA, USA, June 2002, pp. 117–120.
12. C.S. Lin, P.S. Wu, M.C. Yeh, J.S. Fu, H.Y. Chang, K.Y. Lin, and H. Wang, Analysis of multiconductor coupled-line marchand baluns for miniature MMIC design, *IEEE Trans Microwave Theory Tech* 55 (2007), 1190–1199.
13. R. Mongia, I. Bahl, and P. Bhartia, *RF and microwave coupled-line circuits*, Artech House, Norwood, MA, 1999.
14. D. Palombini, S. Arena, T. Cavanna, and E. Limiti, Compact sub-harmonic mixer for Q-band satellite communications, In: *Proceedings of the 9th European Microwave Integrated Circuits Conference*, Rome, Italy, October 2014, pp. 61–64.

© 2016 Wiley Periodicals, Inc.

BI-BAND FRESNEL REFLECTARRAY FOR UNMANNED AERIAL SYSTEM (UAS)-SATELLITE COMMUNICATION

O. Ba, J. Lanteri, C. Migliaccio, and W. Menzel

LEAT—UNS—CNRS UMR 7248 Université Nice-Sophia Antipolis—CNRS Bâtiment Forum Campus Sophi@Tech, 930 Route Des Colles, Sophia Antipolis, 06903; Corresponding author: claire.migliaccio@unice.fr

Received 28 August 2015

ABSTRACT: This article describes the design of a passive Bi-band Fresnel reflectarray (20–30 GHz). It is focused on the design of the reflecting panel of the reflectarray. Two different primary feeds will be used at 20 and 30 GHz, respectively for demonstrating the proposed concept. Nevertheless, in the final design a switched primary feed will have to be used. The dual operation band is obtained with multiple resonant elementary cells. Although the paper deals with linearly polarized primary feed, an interesting property of these cells is that they also work with circular polarization. Moreover, a phase correction based on Fresnel zones is used in order to ensure the best tradeoff between simplicity and radiating performance. Finally, the reflecting panel is made and radiation pattern and gain measurements are shown. © 2016 Wiley Periodicals, Inc. *Microwave Opt Technol Lett* 58:1025–1028, 2016; View this article online at wileyonlinelibrary.com. DOI 10.1002/mop.29730

Key words: reflectarray; unmanned aerial system; satellite communication

1. INTRODUCTION

UAS-satellite communications are studied nowadays. The objective is to replace airplane or helicopters in harsh environment by UAS for different applications such as Survey UAS communication for

fire prevention and coastal zone survey. A 20-GHz frequency band for the downlink and 30-GHz band for the uplink are used [1,2]. For this system, the antenna has to be light, to provide a directive radiation pattern and to work at high frequencies. Printed quasi-optical antennas are good candidates to satisfy these constraints. That is why, a printed Fresnel reflectarray antenna had been chosen. In spite of active solutions were recently proposed [3,4], we propose a fully passive single layer solution for ease of fabrication and power consumption in order to obtain a low cost antenna. Multi-resonant elementary cells [5,6] associated to Fresnel reflectarray [7] were studied. First, we describe how the elementary cell works, then we explain the principle of Fresnel reflectarray and finally simulations and measurement of a demonstrator are shown.

2. ELEMENTARY CELL

The reflectarray surface is divided into elementary cells having the same size ($\lambda/2 \times \lambda/2$ at 20 GHz) but four disk or ring-based patches geometries are used: disk, ring patch, combination of ring and disk or double ring. These geometries combine several advantages:

- Disk or ring-based patches are known to have multiple resonances and we can take advantage of this to obtain multiple frequency operation
- The phase reflected by a given ring-based patch is the same whether the primary feed is linearly or circularly polarized. As a consequence the same reflecting panel can be used for linear and circular polarizations.

The ring patches are known for their multiple resonances. The lower frequency can be adjusted by outer diameter of the ring and higher frequency by inner diameter. We also want to keep dimensions compatible with standard printed circuits techniques, that is, no dimension should be smaller than 100 μm . Therefore, we need to add a disk or another ring inside the first one to reach the different required phases at 20 and 30 GHz. The variation of the phase versus frequency for the different kinds of elementary cell is presented in Figure 1. The substrate used here is Rogers Duroid substrate (ϵ_r : 2.2, thickness: 768 μm).

In Figure 1, we observe that the disk patch is resonant only at lower frequency, but in the same time the second resonance

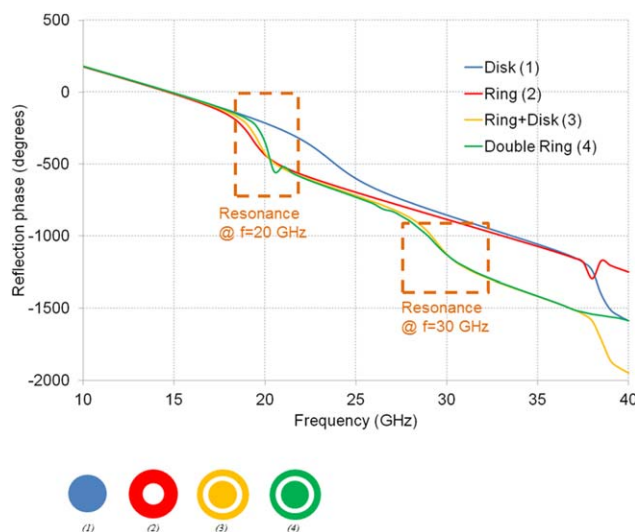


Figure 1 Multi-resonant elementary cell. (1) Disk, (2) ring, (3) ring+disk, (4) double ring. [Color figure can be viewed in the online issue, which is available at wileyonlinelibrary.com]

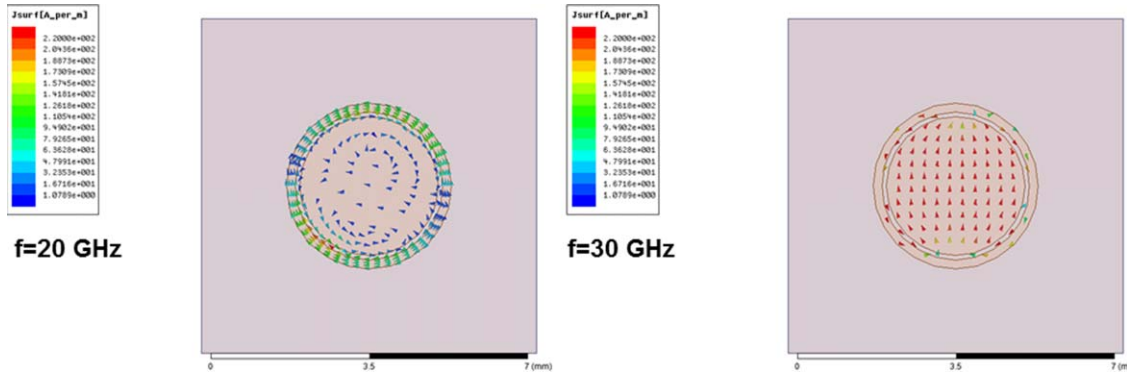


Figure 2 Current distribution for the ring + disk patch at 20 and 30 GHz. [Color figure can be viewed in the online issue, which is available at wileyonlinelibrary.com]

is far away from 30 GHz. The ring has to be modified in order to obtain the resonant frequency at 30 GHz. It is done by adding a small disk inside the ring. However we still cannot obtain all the phase shifts necessary to have the full Fresnel reflectarray phase range, therefore we also use another kind of patch composed of two rings.

To illustrate the patch behavior versus frequency, the current distribution is shown in Figure 2 at 20 and 30 GHz. The incident electrical field is vertical. Currents on the disk patch are parallel to electrical field at 30 GHz. This means that the ring has no influence at this frequency. At 20 GHz, the current is mainly concentrated on the ring patch with a symmetrical distribution with respect to the two minima. Without the disk patch, the minimum would be located along the incident electric field. It means that disk and ring patches are coupled at this frequency and this explains why it is possible to obtain new values of the resonant frequency compared to the ring or the disk alone.

2.1. Fresnel Reflector

The main equations for the Fresnel zones are recalled here.

$$r_n = \sqrt{\frac{2 \cdot n \cdot f \cdot \lambda}{P} + \left(n \cdot \frac{\lambda}{P}\right)^2} \quad (1)$$

With r_n the outer radius of the n th zone,

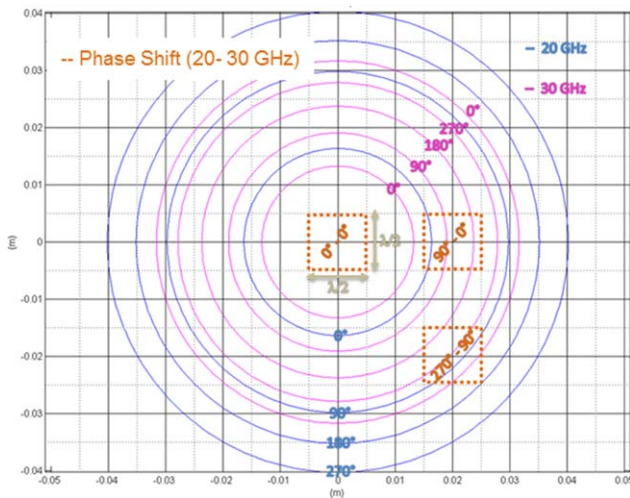


Figure 3 Bi-band Fresnel zones. [Color figure can be viewed in the online issue, which is available at wileyonlinelibrary.com]

$$n = 1, 2, 3, \dots,$$

f : focal length

P : Number of Fresnel zones

$$\varphi_n = \frac{(n-1) \cdot 2\pi}{P} \text{ mod } 2\pi \quad (2)$$

With: φ_n phase shift of the n th cell,

$$n = 1, 2, 3, \dots,$$

P : Number of Fresnel zones

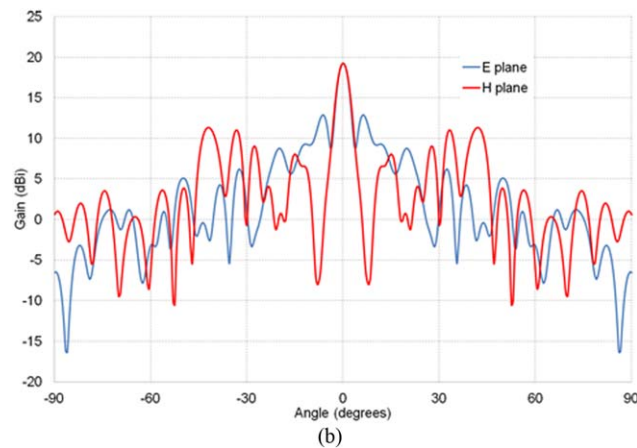
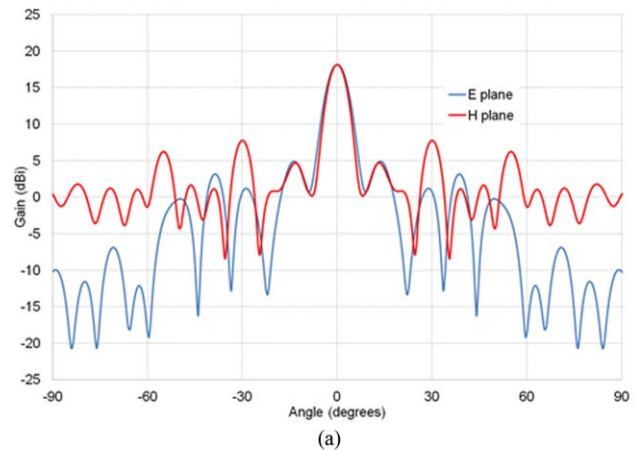


Figure 4 21×21 Fresnel reflectarray radiation pattern simulation. (a) E and H planes at 20 GHz, (b) E and H planes at 30 GHz. [Color figure can be viewed in the online issue, which is available at wileyonlinelibrary.com]

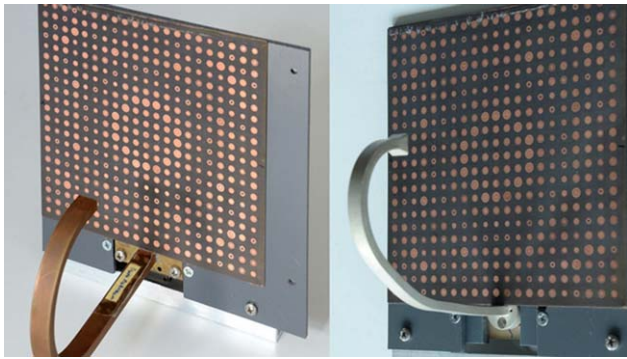


Figure 5 Fresnel reflectarray prototypes. [Color figure can be viewed in the online issue, which is available at wileyonlinelibrary.com]

Greater P is, better will be the phase correction (close of a classical reflector described in [1]). The main advantage of Fresnel reflectarray over classical reflectarray (point to point phase correction) is that only P different elements are required to form the phase front. This greatly simplifies the conception and the fabrication of the reflecting panel. Of course the phase compensation is less accurate and the gain is decreased compared to the point to point phase compensation, but an optimum between manufacturing ease and radiation efficiency is obtained for $P = 8$ [6].

However, with a focal over diameter ratio (F/D) equals to 0.5, the space between two consecutive radiuses become quickly smaller to be able to insert elementary cells with a number of Fresnel zones P equal to 8. That is why, we choose P equals to 4 (quarter wavelength correction).

A 21×21 quarter wavelength Fresnel reflectarray with a centered primary feed and an F/D ratio equal to 0.5 is simulated with Ansys HFSS [8].

Based on the distribution law of Fresnel zones, the number of phase compensation cycles (360°) is repeated more often at 30 GHz than 20 GHz for a same array size (Figure 3). The consequences are a greater number of zones at 30 GHz than 20 GHz and for a given position, and the phases to compensate at 20 and 30 GHz are different most of time. Theoretically, a $1/4$ wavelength Fresnel reflectarray works with four different patches, but here, we need 16 different patches. Some examples are presented Figure 1. Patches sizes are chosen in order to obtain the best tradeoff between the desired phases at 20 and 30 GHz. In its last configuration, the reflectarray has two kinds

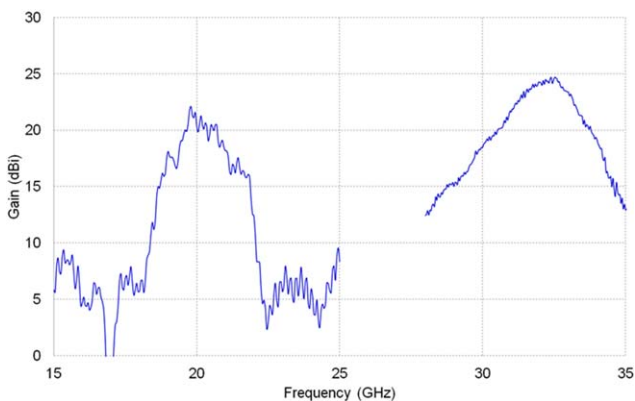


Figure 6 Gain measurement versus frequency. [Color figure can be viewed in the online issue, which is available at wileyonlinelibrary.com]

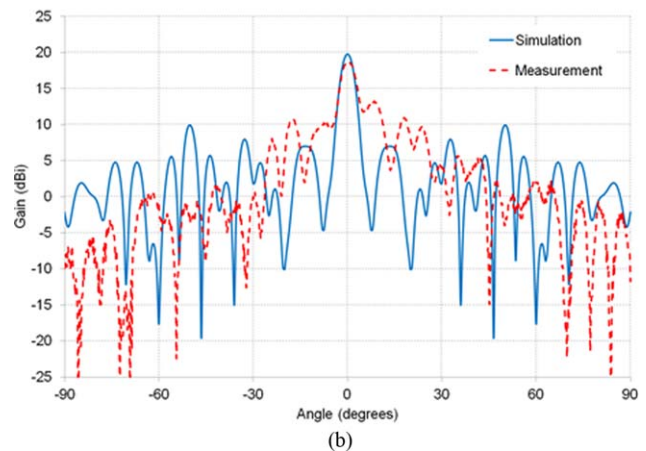
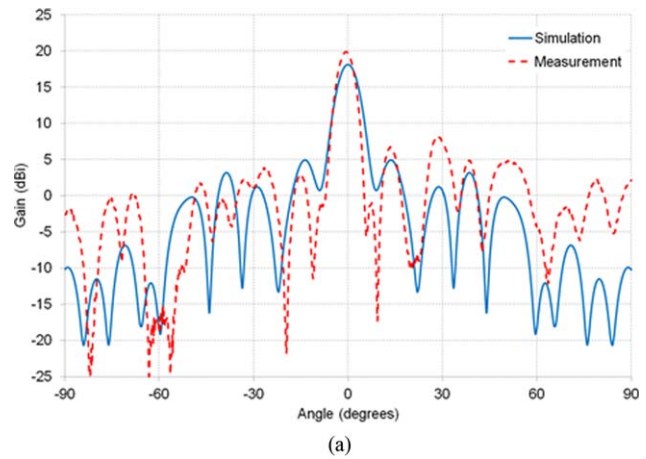


Figure 7 Comparison between simulations and measurement for 21×21 Fresnel reflectarray. (a) E plane at 20 GHz, (b) E plane at 30 GHz. [Color figure can be viewed in the online issue, which is available at wileyonlinelibrary.com]

of unit cells: ring+ disk (358 patches) and double ring patches (83 patches). A study was done for the estimation of the phase error by zone and frequency. The zone ($0-180^\circ$) which represents 10% from the total number of patches has the higher phase error. At 20 GHz, this error is equal to 18° , and at 30 GHz it is 38° . In the other zones, the errors do not exceed 25° . It represents more or less $1/4$ of the phase correction, so it might decrease slightly the radiation efficiency.

2.2. Simulations

The previous Fresnel Reflectarray is simulated with Ansys HFSS (Fig. 4). The primary feed is a standard open-ended waveguide WR-42 at 20 GHz and WR-28 at 30 GHz. Gains are 20 dBi and 18.5 dBi at 20 and 30 GHz, respectively.

2.3. Measurement

The reflecting panel of the reflectarray was fabricated in the LEAT, University Nice Sophia Antipolis and assembled and measured at University of Ulm. The reflectarray panel with both primary feeds at 20 and 30 GHz is shown on Figure 5. The primary feed in Ka-band is a small horn antenna.

The gain measurements are presented in Figure 6 and demonstrate the bi-band performance of the reflectarray. Measured gains are in good agreement with simulation results (20.5 dBi at 20 GHz and 18.5 dBi at 30 GHz). Simulated and measured radiation patterns (E plane) at 20 and 30 GHz are shown in Figure 7.

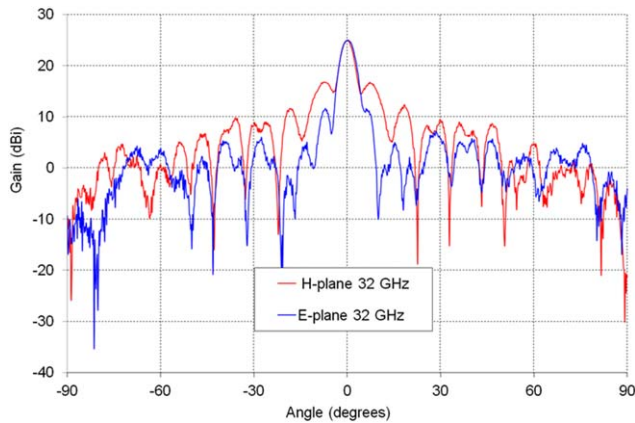


Figure 8 Measured radiation pattern of 21×21 Fresnel reflectarray at 32 GHz. [Color figure can be viewed in the online issue, which is available at wileyonlinelibrary.com]

The difference between simulation and measurement results observed at 30 GHz are due to primary sources slightly different in simulation and measurement.

In Figure 6, we can observe that the optimum frequency is 32 GHz (measured gain equals to 25 dBi). We can explain this result by the tradeoff between reflection phase by unit cell at 20 and 30 GHz that leads to errors compared to theoretical values of the Fresnel zones. More precisely, 10% of the patches at 30 GHz have a phase error of 38° . The tradeoff has more bad effects at this frequency. The radiation pattern was measured at the optimum frequency (32 GHz) and is presented in Figure 8.

3. CONCLUSION

An original passive Fresnel Reflectarray was designed and realized for a bi-band satellite communication application. The bi-band behavior is obtained by using multi resonant elementary cells such as double ring patches and ring + disk patches. These structures have the benefit of being single layer and are easy to produce. The gain measurement shows that the antenna works correctly at 20 and 30 GHz with only small difference with simulations. The need to have a tradeoff between the reflection phases by elementary cells at 20 and 30 GHz shifts the maximum gain at higher frequency.

REFERENCES

1. J.M. Baracco, P.P. Ratajczak, P. Barachat, and G. Toso, Dual frequency Ka-band fresnel reflectors, In: IEEE International Symposium on Antennas and Propagation (APSURSI), Spokane, WA, 2011, pp. 2187–2190.
2. A. Kohmura, J. Lanteri, F. Ferrero, C. Migliaccio, S. Futatsumori, and N. Yonemoto, Ka-band beam switchable fresnel reflector, International Symposium on Antennas and Propagation (ISAP), Nagoya-Japan, 2012, pp. 535–538.
3. S.V. Hum, M. Okoniewski, and R.J. Davies, Realizing an electronically tunable reflectarray using varactor diode-tuned elements, IEEE Microwave Wireless Compon Lett 15 (2005), 422–424.
4. C. Guclu, J. Perruisseau-Carrier, and O. Aydin Civi. In, “Proof of Concept of a Dual-band Circularly-polarized RF MEMS Beam-Switching Reflectarray”, Project report.
5. N. Misran, R. Cahill, and V.F. Fusco, Design optimisation of ring elements for broadband reflectarray antenna, IEE Proc Microwave Antennas Propag 150 (2003), 440–444.
6. B.D. Nguyen, C. Migliaccio, C. Pichot, N. Yonemoto, and K. Yamamoto, W-band fresnel zone plate reflector for helicopter collision avoidance radar, IEEE Trans Antennas Propag 55 (2007), 1452–1456.

7. D.M. Pozar, S.D. Targonski, and H.D. Syrigos, Design of millimeter wave microstrip reflectarrays, IEEE Trans Antennas Propag 45 (1997), 287–296.
8. Ansys-HFSS. Available at: <http://www.ansys.com/Products/Simulation+Technology/Electromagnetics/High-Performance-Electronic+Design/ANSYS+HFSS>

© 2016 Wiley Periodicals, Inc.

HALF HEXAGONAL BROADBAND HIGH GAIN MICROSTRIP PATCH ANTENNA FOR MOBILE AND RADAR APPLICATIONS

Kalyan Mondal and Partha Pratim Sarkar

Department of Engineering and Technology Studies (DETS)
University of Kalyani, Kalyani, Nadia 741235, West Bengal, India;
Corresponding author: kalyankgec@gmail.com

Received 31 August 2015

ABSTRACT: This article presents the design of a broadband microstrip patch antenna for wireless communication. The proposed antenna consists of a radiating patch on one side of a dielectric substrate which has a ground plane on the other side. A half hexagonal microstrip patch antenna is designed using PTFE substrate with dielectric constant 2.4 and thickness $h = 1.6$ mm. To enhance the bandwidth, rectangular slots are incorporated on the ground plane of the half hexagon patch. The proposed antenna works within the frequency range of 2.0–11.5 GHz which exhibits 141% bandwidth with a peak gain of 6.2 dBi. © 2016 Wiley Periodicals, Inc. Microwave Opt Technol Lett 58:1028–1032, 2016; View this article online at wileyonlinelibrary.com. DOI 10.1002/mop.29726

Key words: half hexagonal patch; broadband; high gain; mobile and radar applications

1. INTRODUCTION

The mobile Bluetooth technology provides short range of wireless connections between electronic devices like computers, mobile phones, and many others. The mobile communication systems are growing very rapidly [1,2]. Microstrip patch antennas are very demandable due to low real estate, low profile or size, low cost of fabrication and ease to radiate the power with feeding network. There are some drawbacks like narrow

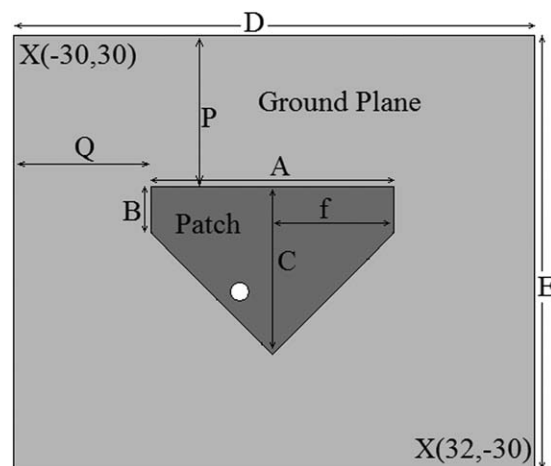


Figure 1 Half hexagonal conventional patch antenna